Ref. 4

538305

AIAA 2000-3955

Design-Filter Selection for H2 Control of Microgravity Isolation Systems: A Single-Degree-of-Freedom Case Study

R. David Hampton
University of Alabama in Huntsville
Huntsville, AL

Mark S. Whorton
NASA Marshall Space Flight Center
Huntsville, AL

AIAA Guidance, Navigation, and Control Conference & Exhibit
14–17 August 2000
Denver, Colorado

AIAA-2000-3955

Design-Filter Selection for H2 Control of Microgravity Isolation Systems: A Single-Degree-of-Freedom Case Study

R. David Hampton*
University of Alabama in Huntsville, Huntsville, Alabama

Mark S. Whorton†
NASA Marshall Space Flight Center, Huntsville, Alabama

ABSTRACT

Many microgravity space-science experiments require active vibration isolation, to attain suitably low levels of background acceleration for useful experimental results. The design of state-space controllers by optimal control methods requires judicious choices of frequency-weighting design filters. Kinematic coupling among states greatly clouds designer intuition in the choices of these filters, and the masking effects of the state observations cloud the process further. Recent research into the practical application of H_2 synthesis methods to such problems, indicates that certain steps can lead to state frequency-weighting design-filter choices with substantially improved promise of usefulness, even in the face of these difficulties. In choosing these filters on the states, one considers their relationships to corresponding design filters on appropriate pseudo-sensitivity- and pseudo-complementary-sensitivity functions. This paper investigates the application of these considerations to a single-degree-of-freedom microgravity vibration-isolation test case. Significant observations that were noted during the design process are presented, along with explanations based on the existent theory for such problems.

INTRODUCTION

The isolation of microgravity space-science experiments from the disturbances of manned space platforms, requires active vibration isolation; passive isolation alone is incapable of providing the desired levels of disturbance attenuation [1, 2, 3, 4, 5]. In designing controllers for these systems, it is convenient to use a state-space description for the system dynamics, along with optimal controls methods (e.g., H_2, H_∞, or mixed-norm), since these modern approaches facilitate the design of robustly stabilizing controllers in the case of multi-degree-of-freedom (MDOF) systems.

Controller-design difficulties can arise, however, due to kinematic coupling among states [6]. Such coupling exists, for example, when relative position and relative velocity are both chosen as states, since the latter is the time derivative of the former. In particular, state kinematic coupling can lead, innocuously, to *conflicting* design-filter weights. These in turn can lead to numerically ill-conditioned regulator and estimator Riccati equations, and to a loss of intuition in the design process. State kinematic coupling can also lead to *redundant* design-filter weights, which can lead in turn to an unnecessary increase in controller dimensionality, with a consequent increase in the complexity of controller implementation.

For the microgravity vibration isolation problem, certain state choices permit kinematically decoupled filter selections. It has been shown [6] that relative position, relative velocity, and absolute acceleration are good state choices for purpose of kinematic decoupling. With these states, the cheap-control performance index can be expressed in terms of an appropriate transmissibility (pseudo-complementary-sensitivity) function $T_{s^2X,\, s^2D}$ and a pseudo-sensitivity function $S_{s^2X,\, s^2D} = I - T_{s^2X,\, s^2D}$, for a system having as input the unisolated-platform (ISS, or "stator") acceleration, and as output, the isolated-platform (ISPR, or "flotor") acceleration. State frequency-weighting filters can then be effectively related to the pseudo-sensitivity- and pseudo-complementary-sensitivity-function frequency-weighting filters, to inform the choice of state frequency-weighting design-filters for loop shaping.

In light of these insights, a reasonable design approach emerges [6, 7]:

(1) Choose the pseudo-sensitivity-function frequency-weighting filter shape(s) for good nominal performance at low frequencies. By "good nominal performance" for the microgravity isolation problem, one means unit transmissibility, for the nominal

---

*Aerospace Engineer, Member AIAA

†Associate Professor of Mechanical Engineering, Member AIAA

plant, to indirect acceleration disturbances below a corner frequency driven by rattle-space constraints [8, 9].
(2) Choose the pseudo-complementary-sensitivity frequency-weighting filter shape(s) for good nominal performance in intermediate and higher frequencies. By "good nominal performance" in these regions, one means rapid roll-off (for *indirect* acceleration disturbances, i.e., disturbances transmitted indirectly through the umbilicals) leading to low acceleration transmissibilities above the corner frequency, for the nominal plant.
(3) Choose frequency-weighting filters to force the controller to "turn off" [i.e., to add negligible energy into the closed-loop (CL) system] above frequencies of interest. One accomplishes this by simultaneously (i) choosing state (or corresponding pseudo-sensitivity- and pseudo-complementary-sensitivity-function) design-filter weightings that place minimal demands for control action at higher frequencies, and (ii) choosing controller design-filter weightings that exact heavy control penalties in that frequency range. This will mean that little control action is requested at higher frequencies, and that such control as is requested is of prohibitive cost.

Reference [6] developed a basis for judicious selection of pseudo-sensitivity- and pseudo-complementary-sensitivity-function frequency weightings; the present paper studies in some detail the results of applying the above design approach to a single-degree-of-freedom (SDOF) test case, for a reasonable set of design objectives.

SDOF TEST CASE

Arrangement and description

Consider a one-dimensional spring-mass-damper isolation system having the arrangement depicted in Figure 1, where d and x are, respectively, the rack and experiment displacements from their equilibrium (relaxed-umbilical) positions.

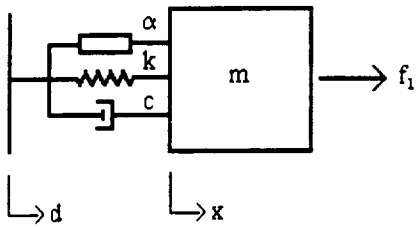

Figure 1. A SDOF Microgravity Isolator

The system parameters are as follows:

actuator current-to-force gain:
$\alpha = 0.2248$ lbf/amp = 1 N/amp,

umbilical stiffness:
$k = 1.5$ lbf/ft = 21.89 N/m,

flotor mass:
$m = 75$ lbm = 2.311 slug = 34.05 kg,

damping:
$c = 0.0374$ lbf · s/ft = 0.1638 N · s/m, and

damping factor:
$\zeta = 0.01$.

The system has a natural frequency of $\omega_n = 0.1277$ Hz and a damped natural frequency of $\omega_d = \omega_n\sqrt{1-\zeta^2} = 0.1277$ Hz. Assume that the actuator is linear, and that it is capable of developing a maximum force of four newtons, so that a control current of four amps corresponds to the upper limit of its linear range.

Equations of motion

From Figure 1 the equation of motion (EOM) for the system is $f_1 - k(x-d) - c(\dot{x}-\dot{d}) + \alpha u = m\ddot{x}$. (1)
Define the following states:

relative position: $z_1 = x - d$, (2)

relative velocity: $z_2 = \dot{x} - \dot{d}$, (3)

and (lowpass-filtered) absolute acceleration:

$$Z_3(s) = \left(\frac{\omega_h}{s+\omega_h}\right) s^2 X(s). \quad (4)$$

Then the EOMs can be written in standard state-space form $\dot{\underline{z}} = A\underline{z} + Bu + E\underline{f}$, (5)

where $\underline{z} = \begin{Bmatrix} z_1 \\ z_2 \\ z_3 \end{Bmatrix}$ and $\underline{f} = \begin{Bmatrix} \ddot{d} \\ f_1/m \end{Bmatrix}$. (6, 7)

Open-loop transfer functions

The open-loop (OL) system has the following transfer-function description:

$$s^2 X(s) = \left(\frac{2\zeta\omega_n s + \omega_n^2}{s^2 + 2\zeta\omega_n s + \omega_n^2}\right) s^2 D(s) + \left(\frac{s^2}{s^2 + 2\zeta\omega_n s + \omega_n^2}\right) F(s) + \left(\frac{\alpha s^2/m}{s^2 + 2\zeta\omega_n s + \omega_n^2}\right) I(s), \quad (8)$$

where the damping factor ζ and the natural frequency ω_n have the usual definitions. The upper-case variables represent the Laplace transforms of the time-domain signals corresponding to the respective lower-case variables, with

$$F(s) = F_1(s)/m. \qquad (9)$$

For the indirect acceleration disturbance $\ddot{d}(t)$, the transfer function to the output acceleration $\ddot{x}(t)$ is $\frac{2\varsigma\omega_n s + \omega_n^2}{s^2 + 2\varsigma\omega_n s + \omega_n^2}$. Note that the corresponding transmissibility plot will have unity gain at low frequencies, a double pole (resonance) at damped natural frequency $\omega_d = 0.1277$ Hz, and a zero at $\frac{\omega_n}{2\varsigma} = 6.4$ Hz, for a slope of -1 at higher frequencies.

For the (mass-normalized) direct disturbance $f(t)$, the transfer function to the output acceleration $\ddot{x}(t)$ is $\frac{s^2}{s^2 + 2\varsigma\omega_n s + \omega_n^2}$. Note that the corresponding transmissibility plot will have a low-frequency slope of +2 (due to the two zeros at the origin), and a double pole (resonance) at ω_d, for a slope of zero and unity gain at higher frequencies.

Available measurements

Assume that relative position and absolute acceleration measurements are available for controller use, as is typically the case. Relative velocity is not directly accessible; this means that an observer will be needed for state reconstruction, in order to use standard optimal-control design methods.

Closed-loop transfer functions

Using all available measurements, the CL system will feed back relative position and absolute acceleration, such that current $I(s) = C_1(s)Z_1(s) + C_2(s)Z_3(s)$. (10)

Using the relationships $Z_1(s) = X(s) - D(s)$ (11)

and $Z_3(s) = s^2 X(s)$, (12)

one can write the following transfer-function description for the CL system:

$$s^2X(s) = \left(\frac{2\varsigma\omega_n s + \omega_n^2 - C_1(s)\left(\frac{\alpha}{m}\right)}{s^2 + 2\varsigma\omega_n s + \omega_n^2 - C_1(s)\left(\frac{\alpha}{m}\right) - C_2(s)\left(\frac{\alpha}{m}\right)\left(\frac{\omega_h}{s+\omega_h}\right)} \right) s^2 D(s)$$
$$+ \left(\frac{s^2}{s^2 + 2\varsigma\omega_n s + \omega_n^2 - C_1(s)\left(\frac{\alpha}{m}\right) - C_2(s)\left(\frac{\alpha}{m}\right)\left(\frac{\omega_h}{s+\omega_h}\right)} \right) F(s). \qquad (13)$$

CONTROL CONSIDERATIONS

Design criteria

The controller, to be acceptable for microgravity vibration isolation, must shape the CL-acceleration transmissibility so as to *pass* low-frequency acceleration disturbances (to accommodate rattle-space constraints), to *reject* intermediate-range acceleration disturbances, to *dampen* resonances, and to "*turn off*" the controller somewhere below frequencies of unmodeled system dynamics. These general requirements can be translated into (1) unit transmissibility (±10%, with zero DC error) to indirect acceleration disturbances for low frequencies, say, below a corner frequency ω_c of about 0.01 Hz; (2) rapid rolloff of transmissibility above the corner frequency, for good attenuation up to about 10 Hz; and (3) controller turn-off (low controller gains) above, say, 100 Hz. For the present case study these were taken as design criteria. It was also required (4) that the actuator current for the CL system not exceed 40 amps per μg at all frequencies, to accommodate the estimated 0.1 μg quasi-steady disturbances without exceeding the linear range of the actuator (4 amps). Note that the transmissibility $T_{s^2X,\, s^2D}$ to indirect acceleration disturbances is the same as the transmissibility T_{XD} from rack displacement $d(t)$ to experiment displacement $x(t)$.

Measurement selection

Observe that, whereas the controller term $C_2(s)$ appears only in the denominators of the two indicated CL transfer functions [Eq. (13)], $C_1(s)$ appears also in the numerator for the indirect-disturbance (i.e., the former) CL transfer function. Observe further that the denominators for the two transfer functions are the same. These facts mean that for any controller using *only* acceleration feedback, i.e., with $C_1(s) = 0$, if the controller has a particular attenuating effect on indirect disturbances $\ddot{d}(t)$ it will also have the identical attenuating effect on (mass-normalized) direct disturbances $f(t)$. The same does not hold for feedback of any other state, or combination of states. Since the only way to increase the attenuation of *both* types of disturbance, for a spring-mass-damper system, is to increase system effective mass (at least, in a frequency-dependent sense), any purely acceleration feedback which improves the attenuation of indirect disturbances must do so by increasing the effective system mass. If the designer uses optimal control methods to design an acceleration-feedback inner loop that meets indirect disturbance-attenuation requirements, he will *automatically* be designing to attenuate direct disturbances as well. He can then add a low-control-authority, relative-position-feedback, outer loop to satisfy any rattle-space

constraints. In other words, the above state- and measurement selections allow the designer to devote his efforts to attenuating only the indirect acceleration disturbances. If he succeeds in that task, he will also attenuate direct disturbances. And since the successful controller adds effective mass to the system, it will tend to improve, rather than to degrade, system stability robustness.

CONTROLLER DESIGN (ACCELERATION-FEEDBACK LOOP)

Design strategy

Various acceleration-feedback controllers were developed by (1) using state-frequency-weighting design-filter shapes considered reasonable based on the theory presented in reference [6], then (2) adjusting the filter weights and the noise covariances until (3) the indirect acceleration transmissibility was considered either acceptable or essentially unimprovable, while (4) maintaining the control current at all frequencies less than or equal to 40 amps/μg. All noise inputs were assumed to have flat power spectra.

Design filter selection

The rationale for filter selection was first to choose the desired pseudo-sensitivity- and pseudo-complementary-sensitivity-function filter shapes, based on the design criteria. Then corresponding state-weighting filter shapes were used to begin the acceleration-feedback controller design. Following the notation in reference [6], the state-weighting filter on each of the states $Z_i\ (i = 1, 2, 3)$ is designated below by W_i; the weighting filters on the pseudo-sensitivity- and pseudo-complementary-sensitivity-functions $S_{s^2X,\, s^2D}$ and $T_{s^2X,\, s^2D}$ (relating to the indicated input and output accelerations) are designated, respectively, as V_S and V_T. The following equations [6] describe the relationships among these frequency-weighting filters:

$$V_S = \left[\left(\frac{W_1}{s^2}\right)^* \left(\frac{W_1}{s^2}\right) + \left(\frac{W_2}{s}\right)^* \left(\frac{W_2}{s}\right)\right]^{1/2} \qquad (14)$$

and

$$V_T = W_3 . \qquad (15)$$

Notice from Equation (14) that either W_1 or W_2 can be used alone to match a particular V_S, and that W_3 determines (or is determined by) V_T. The following table, from Reference [6], indicates the correspondences among various reasonable design-filter choices, in graphical form.

Table 1. Reasonable Weighting-Function Candidates

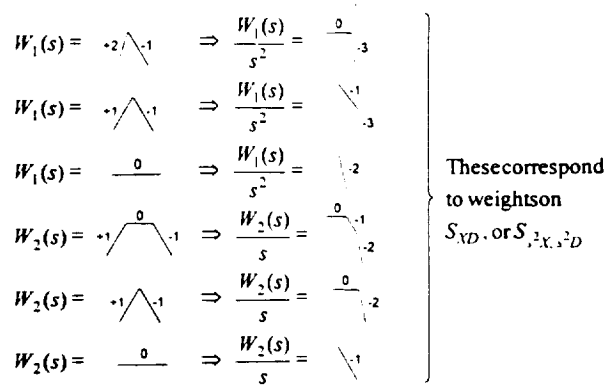

Selected design scenarios

Four design cases follow. In the first two the pseudo-sensitivity function is more heavily weighted than the pseudo-complementary-sensitivity function; in the latter two, the reverse is true. (The implications of this distinction will be discussed in the next major section.)

Case 1: One set of design filters consisted of a bandpass filter (with consecutive legs having slopes of +1, 0, -1) on relative velocity, an open filter (i.e., zero weighting) on relative position, a lowpass filter on absolute acceleration, and a step-up filter (with consecutive legs having slopes of 0, +1, 0) on control current; refer to Figure 2. The corresponding pseudo-sensitivity- and pseudo-complementary-sensitivity-function weightings, V_S and V_T, are shown in Figure 3. Figure 4 presents the OL- and CL plots of the pseudo-complementary-sensitivity function $T_{s^2X,\, s^2D}$ [i.e., OL- and CL transmissibilities to indirect acceleration disturbances $\ddot{d}(t)$]. Figure 5

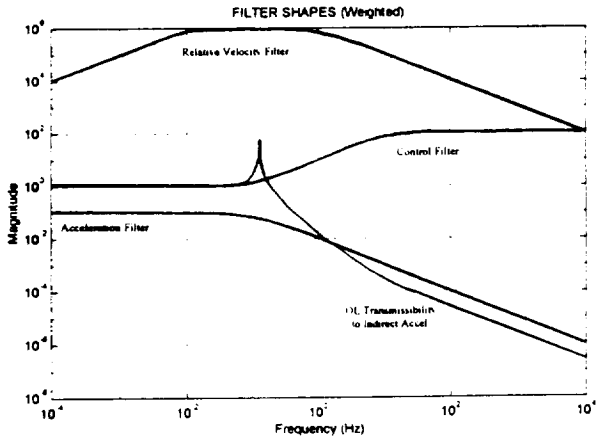

Figure 2. Design Filters for Case 1

shows the OL- and CL transmissibilities to direct (mass-normalized) disturbance $f(t)$. And Figure 6 plots the actuator current versus frequency, for the CL system, in amperes per micro-g.

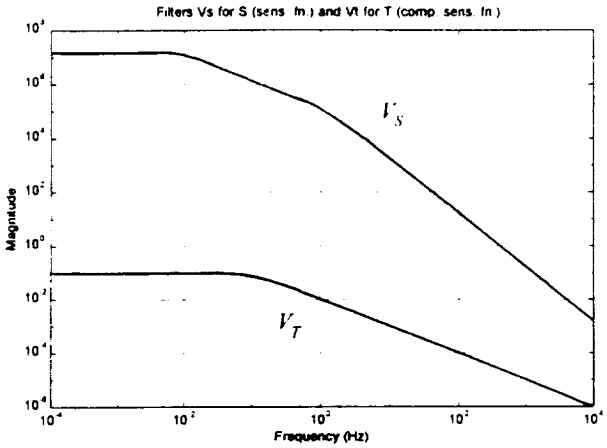

Figure 3. Pseudo-Sensitivity- and Pseudo-Complementary-Sensitivity-Function Weightings for Case 1

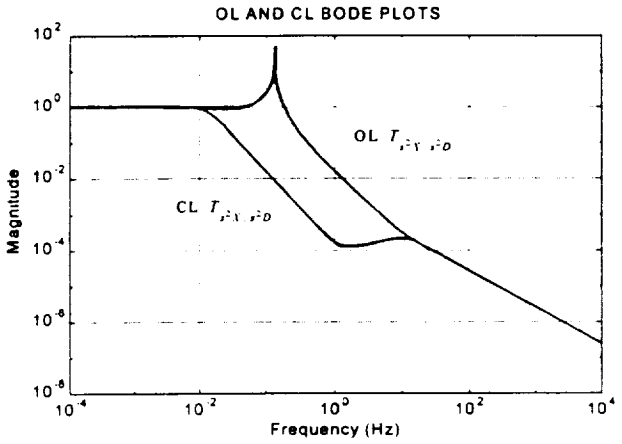

Figure 4. Open-Loop and Closed-Loop Transmissibilities for Indirect Acceleration Disturbances, Case 1

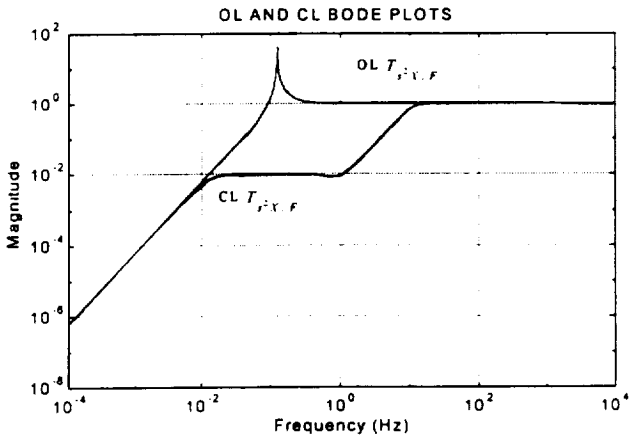

Figure 5. Open-Loop and Closed-Loop Transmissibilities for Direct Acceleration Disturbances, Case 1

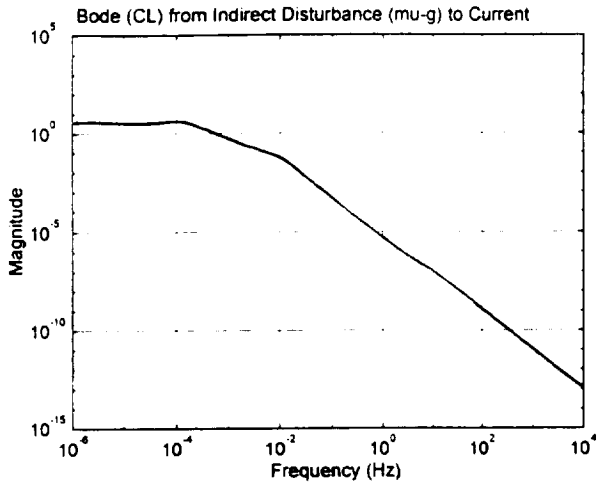

Figure 6. Closed-Loop Actuator Current Versus Frequency (amps/micro-g), for Indirect Disturbances, Case 1

Case 2: A second set of design filters consisted of an open filter (i.e., zero weighting) on relative position, a lowpass filter (consecutive slopes: 0, -1) on relative velocity, a bandpass filter (slopes: +1, 0, -1) on absolute acceleration, and a step-up filter (slopes: 0, +1, 0) on control current; refer to Figure 7. The corresponding pseudo-sensitivity- and pseudo-complementary-sensitivity-function weightings, V_S and V_T, are shown in Figure 8. Figure 9 presents the OL- and CL plots of the pseudo-complementary-sensitivity function $T_{s^2X,\,s^2D}$. Figure 10 shows the OL- and CL transmissibilities to direct (mass-normalized) disturbance $f(t)$. And Figure 11 plots the actuator current versus frequency, for the CL system.

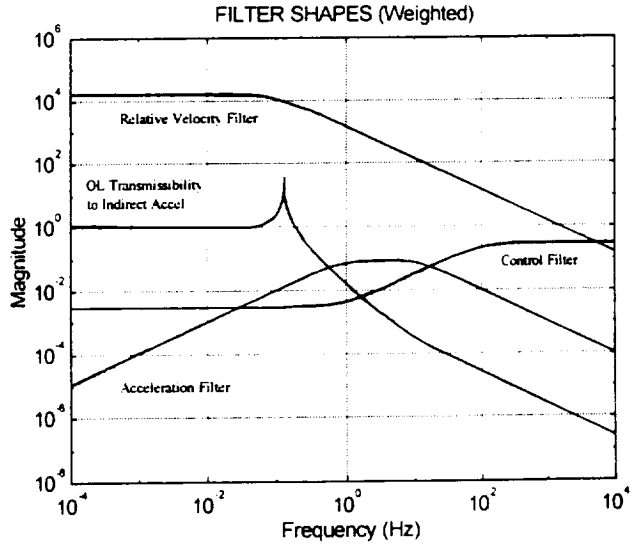

Figure 7. Design Filters for Case 2

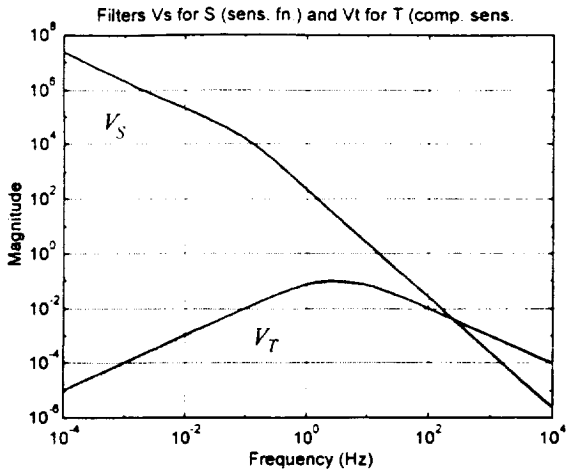

Figure 8. Pseudo-Sensitivity- and Pseudo-Complementary-Sensitivity-Function Weightings for Case 2

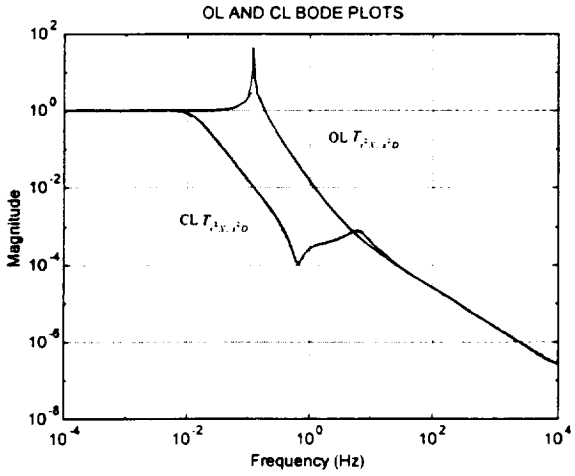

Figure 9. Open-Loop and Closed-Loop Transmissibilities for Indirect Acceleration Disturbances, Case 2

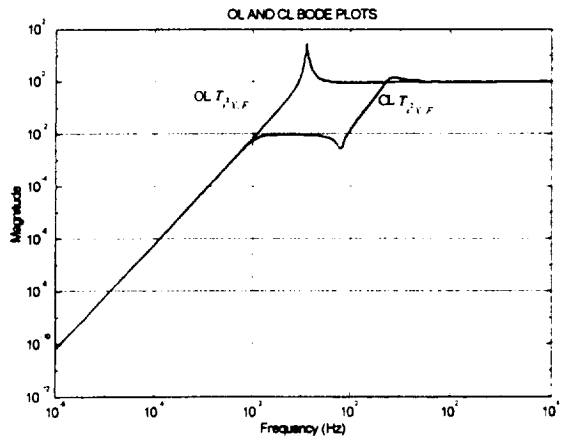

Figure 10. Open-Loop and Closed-Loop Transmissibilities for Direct Acceleration Disturbances, Case 2

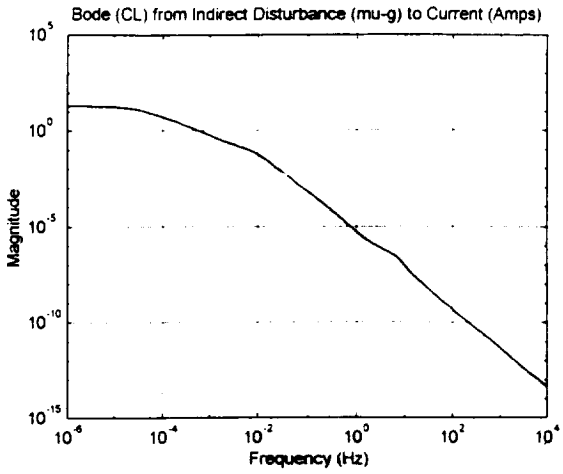

Figure 11. Closed-Loop Actuator Current Versus Frequency (amps/micro-g), for Indirect Disturbances, Case 2

Case 3: A third set of design filters consisted of flat filters (i.e., constant weightings) on relative position and control current, an open filter on relative velocity, and a bandpass filter on absolute acceleration (slopes: +1, 0, -1); see Figure 12. The corresponding pseudo-sensitivity- and pseudo-complementary-sensitivity-function weightings, V_S and V_T, are shown in Figure 13. Figure 14 presents the OL- and CL plots of the pseudo-complementary-sensitivity function. Figure 15 shows the OL- and CL transmissibilities to direct (mass-normalized) disturbance $f(t)$. And Figure 16 plots the actuator current versus frequency, for the CL system.

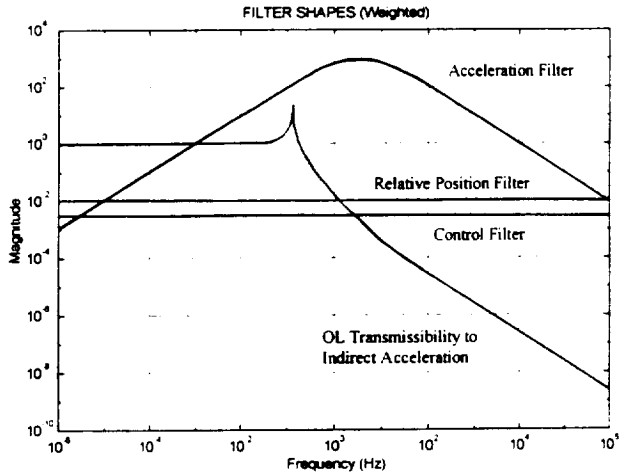

Figure 12. Design Filters for Case 3

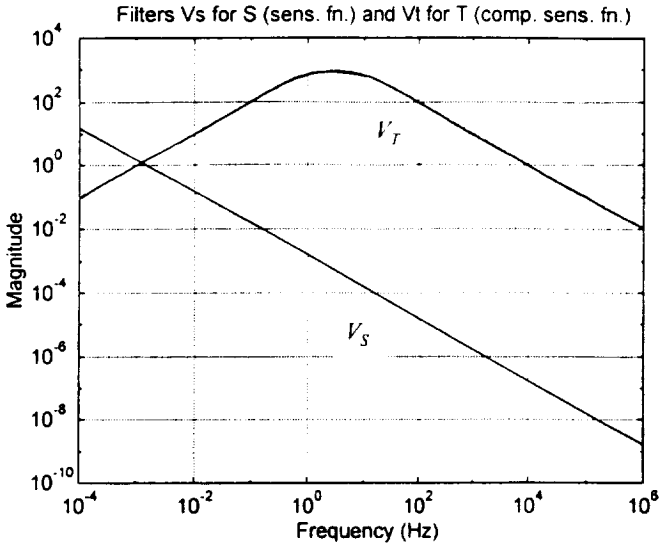

Figure 13. Pseudo-Sensitivity- and Pseudo-Complementary-Sensitivity-Function Weightings for Case 3

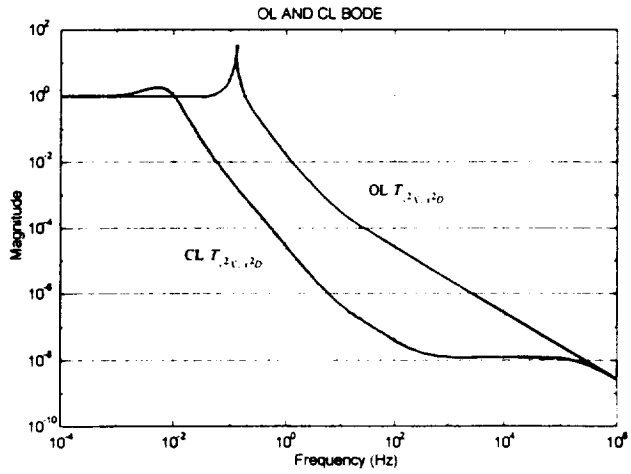

Figure 14. Open-Loop and Closed-Loop Transmissibilities for Indirect Acceleration Disturbances, Case 3

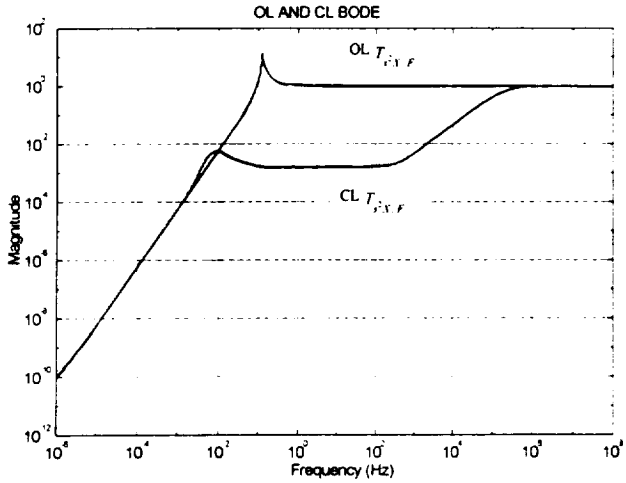

Figure 15. Open-Loop and Closed-Loop Transmissibilities for Direct Acceleration Disturbances, Case 3

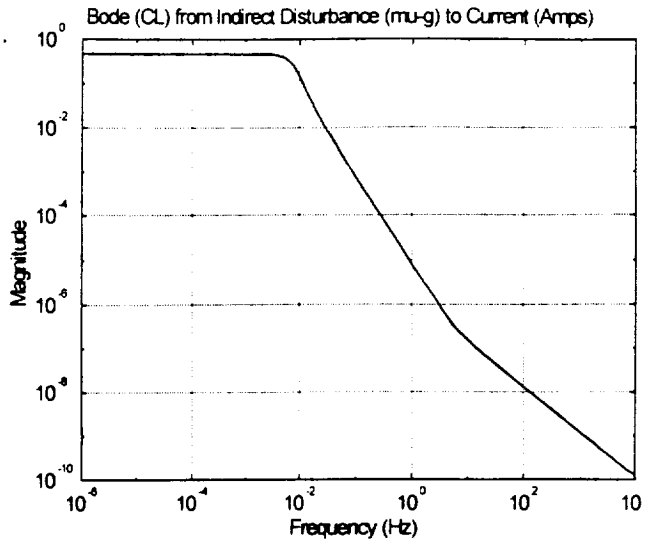

Figure 16. Closed-Loop Actuator Current Versus Frequency (amps/micro-g), for Indirect Disturbances, Case 3

Case 4: A fourth set of design filters consisted of a selection identical in basic shapes to those of Case 3 above, with the exception that the bandpass filter on absolute acceleration had an initial leg with a slope of +2 instead of +1; see Figure 17. The corresponding pseudo-sensitivity- and pseudo-complementary-sensitivity-function weightings, V_S and V_T, are shown in Figure 18. Figure 19 presents the OL- and CL plots of the pseudo-complementary-sensitivity function. Figure 20 shows the OL- and CL transmissibilities to direct (mass-normalized) disturbance $f(t)$. And Figure 21 plots the actuator current versus frequency, for the CL system.

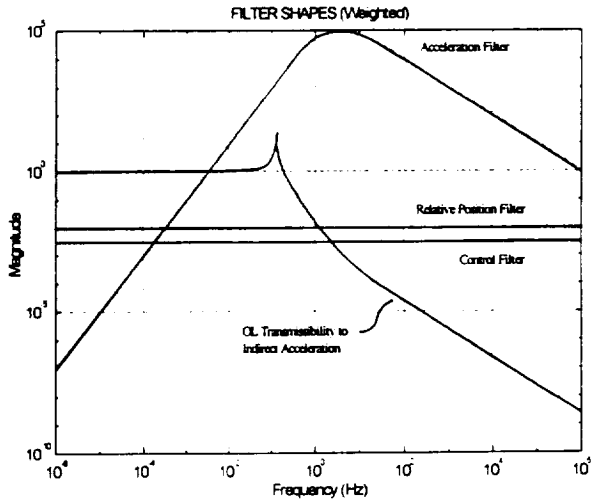

Figure 17. Design Filters for Case 4

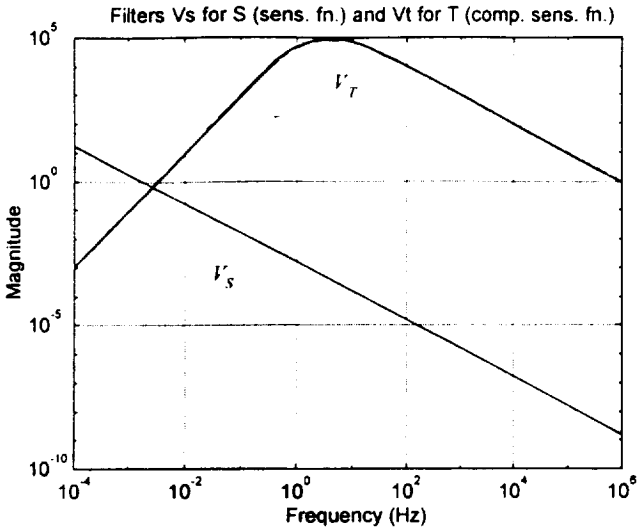

Figure 18. Pseudo-Sensitivity- and Pseudo-Complementary-Sensitivity-Function Weightings for Case 4

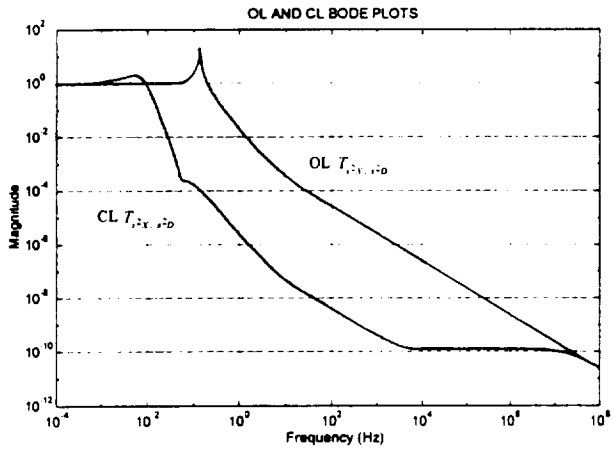

Figure 19. Open-Loop and Closed-Loop Transmissibilities for Indirect Acceleration Disturbances, Case 4

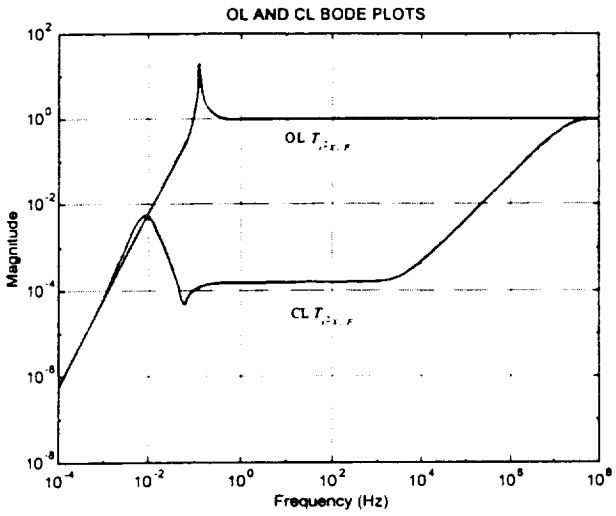

Figure 20. Open-Loop and Closed-Loop Transmissibilities for Direct Acceleration Disturbances, Case 4

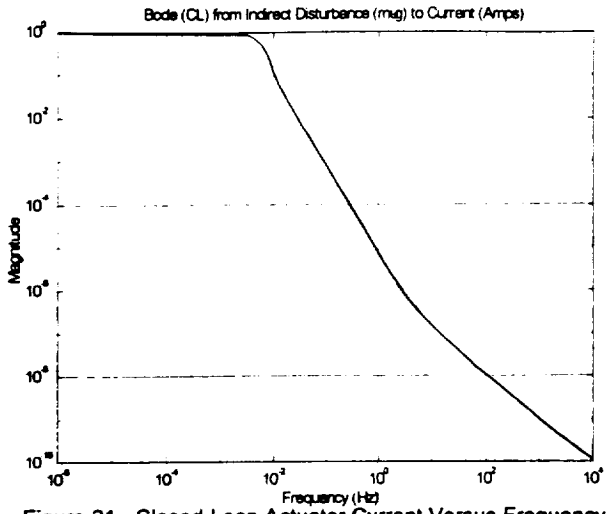

Figure 21. Closed-Loop Actuator Current Versus Frequency (amps/micro-g), for Indirect Disturbances, Case 4

OBSERVATIONS FROM THE CONTROLLER-DESIGN SCENARIOS

Observations related to the regulator

1. A combination of relatively high weighting on control, and relatively low weighting on both the pseudo-sensitivity- and pseudo-complementary-sensitivity functions, leads to controller turn-off at high frequencies.

Remark: The observed effects are a low control current (e.g., see Figure 6) and an eventual rejoining of OL- and CL transmissibilities at high frequencies (e.g., see Figures 4 and 5), when the controller is no longer called upon to act significantly on the system.

2. The rate of transmissibility-plot roll-off, above ω_c, is affected by the frequency weighting V_T on the pseudo-complementary-sensitivity function. In general, the steeper the ascent of the pseudo-complementary-sensitivity-function frequency weighting, the steeper the descent of the CL-transmissibility plot. Figure 14 shows the transmissibility to an indirect acceleration disturbance, with the filter shapes chosen for Case 3; Figure 19 corresponds to Case 4. Note the steeper roll-off in Figure 19, due to the steeper (+2 slope) initial leg of the pseudo-complementary-sensitivity-function weighting (Figure 18).

Explanation: The weighting on the pseudo-complementary-sensitivity function tells the regulator how much effort to put into indirect-disturbance rejection, as a function of frequency.

Remark: The use of an observer often tends to mask this effect with frequency-weighted observation. This masking is due to the fact that frequency-weighted observation typically results in observer poles having time constants of the same

order as those of the regulator poles. With the resultant observer and regulator coupling, either may dominate in affecting the overall controller, depending on the choices of design-filter shapes and weights. It was found that in Cases 1 and 2 the observer tended to dominate; in Cases 3 and 4, the regulator.

3. For a given, reasonable set (e.g., see Table 1) of weighting filters V_S and V_T, the location of ω_c can be adjusted by trading off the respective weightings of the pseudo-sensitivity- and pseudo-complementary-sensitivity functions. In general, increasing the former and decreasing the latter tends to move the corner frequency to the right.

Explanation: These effects are consistent with the observations that the pseudo-sensitivity-function weighting can be viewed as a weighting on relative position, affecting effective stiffness; and that the pseudo-complementary-sensitivity-function weighting is essentially a weighting on acceleration, affecting effective mass. (As with the preceding item, the observer can mask this effect.)

Remark: Multiplying the pseudo-sensitivity- and pseudo-complementary-sensitivity function weightings by a common factor was found to be particularly effective in adjusting the corner frequency. This technique was especially useful in Cases 3 and 4, for which the regulator tended to dominate the observer. Note that multiplying by a common factor has the effect, at any given frequency, of increasing the larger weighting by a greater amount (additively). This raises its additive (though not its proportional) contribution to the quadratic cost, so that the controller-design machinery must focus more attention to its reduction.

4. The regulator gains are not affected by the process- or measurement-noise covariances.

Explanation: This result is expected from the well-known "Separation Principle." The regulator-design Riccati equation is unaffected by process- or measurement noise covariances if all the noise signals are white.

Remark: With colored noise, the dynamics of the respective process- and measurement-noise frequency-weighting filters appear in the generalized plant and, consequently, in the regulator Riccati equation [10]. This additional information does, of course, affect the regulator gains.

Observations related to the observer

1. As acceleration measurement noise is increased, the CL corner frequency (ω_c) moves to the right until, in the limit, the CL Bode plot approaches the OL Bode plot.

Explanation: In effect, when measurement noise increases excessively, the observer loses the ability to reconstruct the states with confidence, and shuts down the feedback controller.

2. The observer gains are not affected if the cost functional contains only flat (simple scalar) weights on *all* state- and control signals. However, if weighting filters W_i are used on any of those signals, the observer gains are affected.

Explanation: This result is expected, again, from the "Separation Principle." The observer-design Riccati equation is unaffected by simple scalar weights on the state- and control signals, provided *none* of these signals is frequency weighted. Any frequency weightings of the state- and control signals, however, appear in the observer Riccati equation and thus affect the observer gains [10].

3. The achievable isolation is greatly improved by using the same frequency-weighting filters for observer design as for design of the regulator.

Explanation: The use of the same frequency weightings for regulator and observer designs allows the observer design machinery to have the same plant information as the controller design machinery. The observer can consequently focus its state-reconstruction efforts optimally.

4. For Cases 1 and 2, increasing the direct-disturbance process-noise covariance lowers ω_c. The range of ω_c that could be achieved by this means alone extends from about 0.0023 Hz to about 0.6 Hz.

Explanation: Consider the state energy term of the cost functional, in the following form:

$$I_Z = (X-D)^*\left[\left(s^2V_S\right)^*\left(s^2V_S\right)\right](X-D) + \left(s^2X\right)^*\left[V_T^*V_T\right]\left(s^2X\right). \tag{16}$$

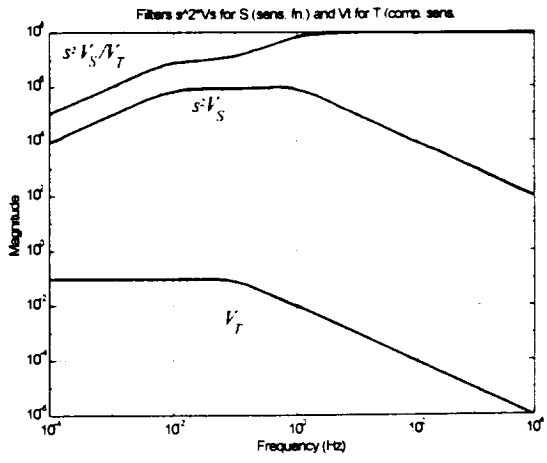

Figure 22. Bode Plots of s^2V_S, V_T, and s^2V_S/V_T, Case 1

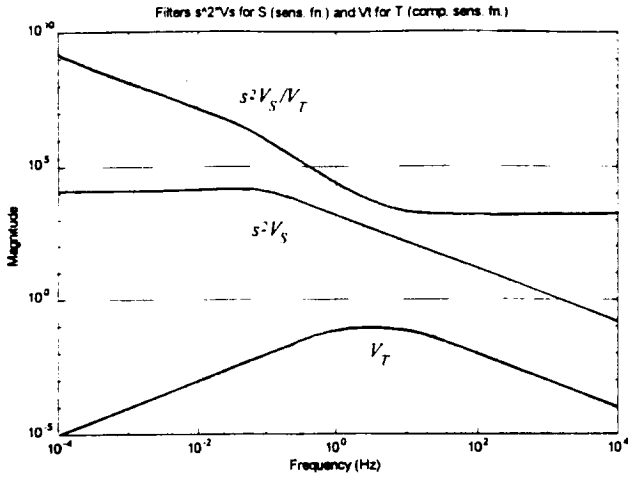

Figure 23. Bode Plots of s^2V_S, V_T, and s^2V_S/V_T, Case 2

Figures 22 and 23 present Bode magnitude plots of s^2V_S, V_T, and s^2V_S/V_T, for Cases 1 and 2, respectively. The plot for s^2V_S/V_T gives a direct measure (assuming cheap control) of the cost of relative-position state Z_1 relative to that of acceleration state Z_3. This relative importance is assigned to the performance index by the state-weightings W_i (see Equations 14 and 15). In each of the first two cases the controller design machinery must focus very heavily on the Z_1 state. To attenuate a direct disturbance, the controller can act to increase (in a frequency-dependent fashion) either effective system mass, via acceleration feedback; or stiffness, via relative-position feedback; or both. The high relative cost of relative-position feedback drives the controller to focus on increasing acceleration feedback. The resultant increase in effective system mass drives the corner frequency down. Since process noise cannot affect regulator gains (see #2 above), these changes in acceleration feedback must be accomplished by changes in the observer gains.

Remarks: Notice here that it is not actually the controller's "assigned" task to attenuate direct disturbances. The given design problem is formulated for accomplishing the attenuation of indirect disturbances. However, an increase in direct disturbance effects an increase in the power of $X-D$, which is heavily weighted through s^2V_S, so that direct-disturbance attenuation is at least indirectly required.

With direct disturbances, the attenuation of most concern to the controller-design machinery (i.e., from the perspective of the state-energy term I_Z) is from mass-normalized direct-disturbance F to $X-D$. Note that F is approximately equal to s^2X for high enough frequencies, i.e., above about 0.1 Hz for the open-loop system, and above about 10 Hz closed-loop.

5. For Cases 1 and 2, increasing the indirect-disturbance process-noise covariance raises ω_c. The range of ω_c that could be achieved by this means, with either of those two designs, extends from about 0.01 Hz to about 6 Hz.

Explanation: Consider again the state energy term in the form of Equation 16, and refer to the plots for s^2V_S/V_T in Figures 22 and 23. Since the relative-position term dominates the cost, an increase in indirect-disturbance energy (for the design-model) requires the controller to focus on minimizing the relative-position state. To accomplish this, the controller can act (in a frequency-dependent fashion) to increase effective stiffness, via increased relative position feedback; to decrease effective mass, via reduced acceleration feedback; or both. The high relative cost of relative-position feedback drives the controller to focus on reducing acceleration feedback. The resultant decrease in effective system mass pushes the corner frequency up. Since process noise cannot affect regulator gains (see #4 above, previous section), these changes in acceleration feedback must be accomplished by changes in the observer gains.

Remarks: Notice that although it is, in fact, the controller's assigned task to attenuate indirect disturbances, it is incorrect here to reason that it could try to do so by *lowering* effective stiffness or by *increasing* effective mass. As indicated in the paragraph above, precisely the opposite is true. The reason lies in the (present designers') choice of a dominant state weighting $\left(s^2V_S\right)$ on relative position Z_1 (Equation 16). Because of this weighting, for indirect disturbances the attenuation of most concern to the controller-design machinery (i.e., from the perspective of the state-energy term I_Z) is really from s^2D to $X-D$. If V_T had been dominant (as it could certainly have been, by designer choice), the indirect disturbance would have had its primary effect on the state-energy cost via acceleration state Z_3. In *that* case the attenuation could have been effected by *lowering* effective stiffness or *increasing* effective mass. The somewhat counterintuitive effect of the controller's reducing effective mass, in response to increased indirect-disturbance power (in the design model), illustrates the design difficulties that sometimes result with kinematic coupling among states.

6. For Cases 3 and 4, changes in the direct- and indirect-disturbance process-noise covariances have negligible effect on ω_c.

Explanation: Consider again the state energy term in the form of Equation 16, and refer to the plots

for $s^2 V_S / V_T$ in Figures 24 and 25. Since for these two cases the acceleration term (i.e., due to V_T) dominates the

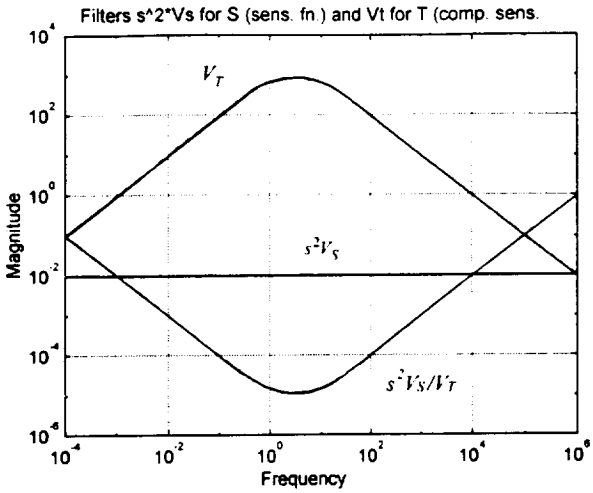

Figure 24. Bode Plots of s^2V_S, V_T, and s^2V_S/V_T, Case 3

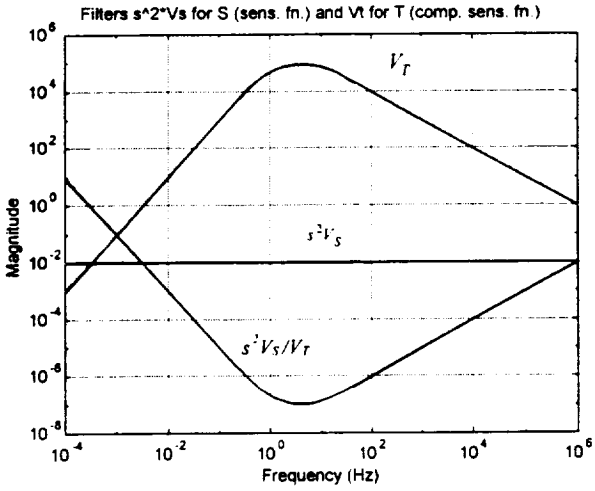

Figure 25. Bode Plots of s^2V_S, V_T, and s^2V_S/V_T, Case 4

cost, an increase in disturbance energy (for the design-model) requires the controller to focus on minimizing the acceleration state. It can only do this (at least, via the observer) by changing the quality of the state observations, in a frequency-weighted sense. In particular, to have much effect on the controller, the observer must make its primary contribution to cost reduction in the region of greatest cost. This region is defined primarily by the band-pass filter V_T, and extends roughly from about 10^{-3} to 10^{4} Hz. It turns out that in this region the observer's reconstruction of the acceleration state is already quite good, and nearly exact in the vicinity of 10^{-2} Hz, so that the observer has little room to effect an improvement. Consequently, the observer can have little effect on ω_c. In summary, for Cases 3 and 4 the dominance of the regulator (due, in turn, to the good quality of acceleration-state reconstruction in the high-cost region) masks the changes in the controller that can be achieved via the process-noise covariances.

Remarks: It should be noted that, for these two cases, ω_c can be moved quite easily, by varying the relative contributions of weighting filters V_S and V_T to the quadratic cost. (See the 3rd observation in the previous section.) It is also worth noting that, although the observer does not affect ω_c appreciably, variations in the disturbance process-noise covariances do change the depth of the "bowl" in the "high-cost" region, as the observations of the acceleration state change in quality.

Additional, general observations

1. Above frequency $\frac{\omega_n}{2\zeta}$ (6.4 Hz) the indirect disturbance transmissibility plot has the expected -1 slope; the direct disturbance transmissibility plot has the expected zero slope.

Explanation: The open-loop system has a zero at $\frac{\omega_n}{2\zeta}$.

2. Pseudo-sensitivity-function weightings not directly achievable (such as pure integrators) can be requested via state frequency weightings. [For example, in Case 2, flat (i.e., constant) weighting on relative velocity, corresponds to a single-integration pseudo-sensitivity-function weighting. As another example (see Table 1), flat weighting on relative position, would correspond to a double-integration pseudo-sensitivity-function weighting.]

3. Considering Item (2) above from another perspective, pseudo-sensitivity-function weightings can be achieved by alternate means, according to the state(s) chosen to be weighted, although the use of an observer will tend to result in controller differences.

CONCLUSION

This paper has studied a test problem for the design of a feedback controller by H_2 synthesis. The particular problem selected treats a single-degree-of freedom microgravity vibration-isolation system, with kinematic state-coupling. State-weighting design filters were chosen based on reasonable choices for pseudo-sensitivity-function and pseudo-complementary-sensitivity-function weightings. Significant observations that were noted during the design process were listed, along with

explanations and correlations to the existent theory for such design problems.

ACKNOWLEDGEMENTS

The authors are grateful for financial support for this research, under the 1998 NASA/ASEE Summer Faculty Fellowship Program, and under a subsequent grant from NASA Marshall Space Flight Center.

REFERENCES

1. Nelson, Emily S., "An Examination of Anticipated g-Jitter on Space Station and Its Effects on Materials Processes," NASA TM-103775, April 1991.
2. DelBasso, S., "The International Space Station Microgravity Environment," AIAA-96-0402, January 1996.
3. "System Specification for the International Space Station," Specification Number SSP41000, Rev. D, Nov. 1, 1995, NASA Johnson Space Center.
4. DeLombard, R., Bushnell, G. S., Edberg, D., Karchmer, A. M., and Tryggvason, B. V., "Microgravity Environment Countermeasures Panel Discussion," AIAA-97-0351, January 1997.
5. Grodsinsky, Carlos M. and Brown, Gerald V., "Nonintrusive Inertial Vibration Isolation Technology for Microgravity Space Experiments," NASA TM-102386, AIAA-90-0741, January 1990.
6. Hampton, R. David and Whorton, Mark S., "An Indirect Mixed-Sensitivity Approach To Microgravity Vibration Isolation: The Exploitation of Kinematic Coupling In Frequency-Weighting Design-Filter Selections," ACC00-AIAA0036, June 2000.
7. Hampton, R. David and Whorton, Mark S., "Frequency-Weighting Filter Selection, for H_2 Control of Microgravity Isolation Systems: A Consideration of the "Implicit Frequency Weighting" Problem," IEEE 99-9184, *IEEE Transactions on Instrumentation and Measurement*, April 2000.
8. Knospe, C. and Allaire, P., "Limitations on Vibration Isolation for Microgravity Space Experiments," *Journal of Spacecraft and Rockets*, Vol. 27, No. 6, Nov.-Dec. 1990, pp. 642-646.
9. Knospe, C. and Allaire, P., "Limits on the Isolation of Stochastic Vibration for Microgravity Space Experiments," *Journal of Spacecraft and Rockets*, Vol. 28, No. 2, March-April 1991, pp. 229-237.
10. Hampton, R. D., Knospe, C. R., Allaire, P. E., and Grodsinsky, C. M., "Microgravity Isolation System Design: A Modern Control Synthesis Framework," *Journal of Spacecraft and Rockets*, Vol. 33, No. 1, January-February 1996, pp. 101-109.